Optimization of a Hot Structure Aeroshell and Nose Cap for Mars Atmospheric Entry

Sarah L. Langston[*]

National Institute of Aerospace, Hampton, Virginia, 23666, USA

Christopher G. Lang[†], Jamshid A. Samareh[‡], and Kamran Daryabeigi[†]

NASA Langley Research Center, Hampton, Virginia, 23681, USA

The National Aeronautics and Space Administration (NASA) is preparing to send humans beyond Low Earth Orbit and eventually to the surface of Mars. As part of the Evolvable Mars Campaign, different vehicle configurations are being designed and considered for delivering large payloads to the surface of Mars. Weight and packing volume are driving factors in the vehicle design, and the thermal protection system (TPS) for planetary entry is a technology area which can offer potential weight and volume savings. The feasibility and potential benefits of a ceramic matrix composite hot structure concept for different vehicle configurations are explored in this paper, including the nose cap for a Hypersonic Inflatable Aerodynamic Decelerator (HIAD) and an aeroshell for a mid lift-to-drag (Mid L/D) concept. The TPS of a planetary entry vehicle is a critical component required to survive the severe aerodynamic heating environment during atmospheric entry. The current state-of-the-art is an ablative material to protect the vehicle from the heat load. The ablator is bonded to an underlying structure, which carries the mechanical loads associated with entry. The alternative hot structure design utilizes an advanced carbon-carbon material system on the outer surface of the vehicle, which is exposed to the severe heating and acts as a load carrying structure. The preliminary design using the hot structure concept and the ablative concept is determined for the spherical nose cap of the HIAD entry vehicle and the aeroshell of the Mid L/D entry vehicle. The results of the study indicate that the use of hot structures for both vehicle concepts leads to a feasible design with potential weight and volume savings benefits over current state-of-the-art TPS technology that could enable future missions.

Nomenclature

ACC	Advanced Carbon-Carbon
CMC	Ceramic Matrix Composite
EDL	Entry, Descent, and Landing
FIAT	Fully Implicit Ablation and Thermal response program
HIAD	Hypersonic Inflatable Aerodynamic Decelerator
LEO	Low Earth Orbit
MSL	Mars Science Laboratory
Mid L/D	Mid Lift-to-Drag
NASA	National Aeronautics and Space Administration
OFI	Opacified Fibrous Insulation
PICA	Phenolic Impregnated Carbon Ablator
RTV	Room Temperature Vulcanizing adhesive
TPS	Thermal Protection System

[*]Research Aerospace Engineer, National Institute of Aerospace, Mail Stop 190, AIAA Member.

[†]Aerospace Engineer, Structural Mechanics and Concepts Branch, Mail Stop 190.

[‡]Aerospace Engineer,Vehicle Analysis Branch, Mail Stop 451, AIAA Associate Fellow.

American Institute of Aeronautics and Astronautics

I. Introduction

The mission to send humans to Mars will require larger payloads to be delivered to the surface of the planet than previously done. This may require novel approaches in space vehicle design, both in the shaping and architectures of the vehicles and materials. Thermal protection systems (TPS) are a requirement for Mars entry systems due to the extreme aerodynamic heating. This aerodynamic heating is exacerbated by the thin atmosphere of Mars, making the TPS of a Mars entry vehicle a potential weight and design driver. The current state-of-the-art in TPS technology uses an ablative material which dissipates heat by ablating and insulates an underlying structure.

Ablators are considered semi-passive thermal management systems. They are a single use TPS, but are able to withstand much higher heating rates than reusable TPS.[1,2] The underlying structure typically consists of an aluminum honeycomb with aluminum or composite facesheets, and the ablator is bonded to the structure using room temperature vulcanizing (RTV) adhesive with or without a strain isolation pad. Ablation is typically used for short duration entry trajectories. The use of ablators manages the thermal loads in multiple ways. Heat is both blocked by ablation and absorbed during the ablation process, as well as exhibiting transpiration cooling effects.[1,2] Ablative TPS was used by the Apollo missions and is in current use on the Orion capsule. Traditionally, ablative TPS has been used on spacecraft sent to the surface of Mars.[3–5] These capsules face much higher heating rates than a lifting body craft such as the Space Shuttle Orbiter. The ceramic tiles used on the Orbiter are a reusable, passive TPS. The Orbiter was a lifting body craft. The entry profile consisted of lower heating rates over a much longer period of time as the craft glided down to Earth. The Apollo and Orion capsules face a ballistic type entry, which is characterized by higher heating rates for a reduced time period.

Hot structures refers to materials that can handle both structural and thermal loads. Potential applications include nose caps, control surfaces, heat shields, and aeroshells. Materials of this type can be used to carry the primary structural loads without any additional thermal protection, such as an ablator or ceramic tile. Hot structures can be used in a passive TPS design, which can withstand high heating rates for long periods of time without a substantial change in geometry. Lightweight high temperature insulation can be used with hot structures to protect the interior when required.[1,2] Because hot structures have little to no change in their outer mold line geometry during use, they can be reused.

Novel vehicle concepts and configurations are necessary to achieve the delivery of large payloads to Mars. Two current examples of vehicle concepts being studied are the Hypersonic Inflatable Aerodynamic Decelerator (HIAD) and mid lift-to-drag (Mid L/D) vehicle geometries.[6] The HIAD concept expands upon the traditional ballistic type entry to the planet that has been used on prior missions, while the Mid L/D concept alters the entry trajectory by use of a lifting body geometry, similar to the Shuttle Orbiter, that will have a shallower trajectory to the surface. The differences in the vehicle geometries and trajectories will produce different heating rates encountered by the vehicles.

The present study sought to compare the use of traditional ablative TPS designs and hot structures on two different vehicle architectures, the rigid nose of a HIAD vehicle and the aeroshell of a mid L/D vehicle. The figures of merit for the comparison would be the areal density and thickness.
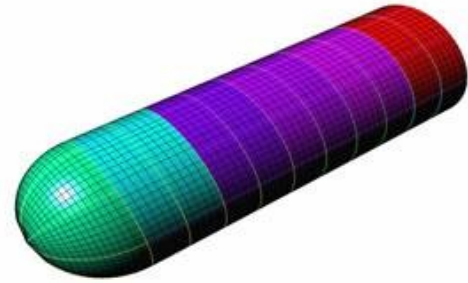
II. Vehicle Designs

HIADs are inflatable heat shields that allow for a larger aeroshell area than could normally be accommodated with current launch vehicles. This opens up many different mission possibilities, both in deep space and low Earth orbit (LEO) return. HIADs use a flexible TPS for the inflated portion of the structure and can use various other forms of TPS for the rigid center structure.[7] An artistic rendering of the HIAD with potential payload placement is seen in Figure 1a.

A potential design for a Mid L/D vehicle can be seen in Figure 1b. For this study, an idealized version of the geometry was used that included a cylindrical body and hemispherical nose with no wings or control surfaces.[8,9] The shape of the aeroshell aligns with the lifting-body type trajectory and presents a different heating profile as compared to the capsule design.
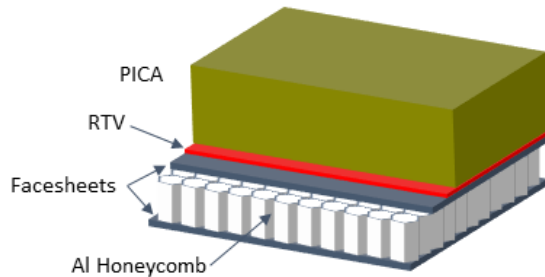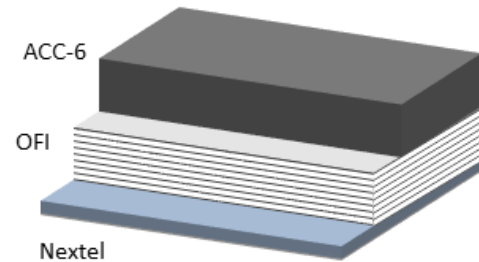
American Institute of Aeronautics and Astronautics

Figure 1: Conceptual designs for (a)[7] HIAD and (b)[10] Mid L/D.

The specific materials chosen for this study are depicted in Figure 2. The materials and layups used are the same for both vehicles. The ablative TPS design consists of an ablator attached to a honeycomb sandwich composite carrier structure. Phenolic impregnated carbon ablator (PICA)[11] was selected because it represents the current state-of-the-art in ablator technology and has been successfully used on the Mars Science Laboratory (MSL) mission to Mars.[3, 4, 12] The PICA is bonded to a carrier structure using RTV-560 adhesive, which has been previously used on spacecraft. The carrier structure consists of graphite facesheets and an aluminum honeycomb core. The ablative TPS stack-up can be seen in Figure 2a. This stack-up mimics the heatshield layup flown on the MSL in terms of the PICA ablator, honeycomb composite carrier structure, and RTV as a bonding agent.[3, 4, 12] The hot structure material chosen was a ceramic matrix composite, specifically advanced carbon carbon (ACC) that has been though six pyrolysis cycles (ACC-6). Behind the ACC-6 is a layer of opacified fibrous insulation (OFI),[13] which is held in place by a layer of Nextel fabric. This stack-up is shown in Figure 2b.

Figure 2: Schematic of the (a) ablative and (b) hot structure designs.

A.   HIAD Geometry

The HIAD vehicle consists of a rigid nose in the center of the vehicle that is surrounded by inflatable tori covered in a flexible TPS material that increases the overall diameter of the vehicle. A conceptual sketch of a cutaway of the HIAD vehicle can be seen in Figure 3. The central rigid nose section was the focus of this study, and is what was modeled. The spherical rigid nose was 9.1 meters in diameter with a seventy-degree cone angle.
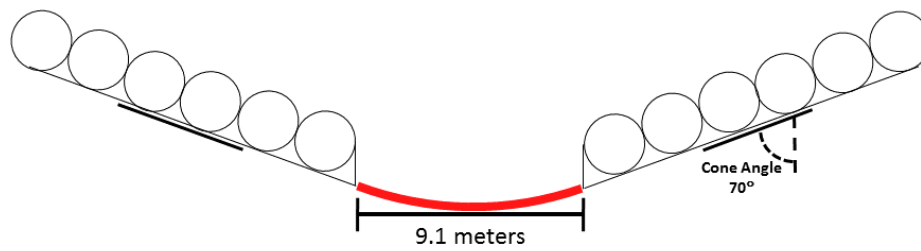
American Institute of Aeronautics and Astronautics

Figure 3: Cross-section of rigid nose concept.

B. Mid L/D Geometry

The Mid L/D vehicle studied has an idealized geometry consisting of a cylindrical body and a hemispherical nose section. The baseline vehicle is thirty meters in length and has a radius of 10 meters, shown in Figure 4.
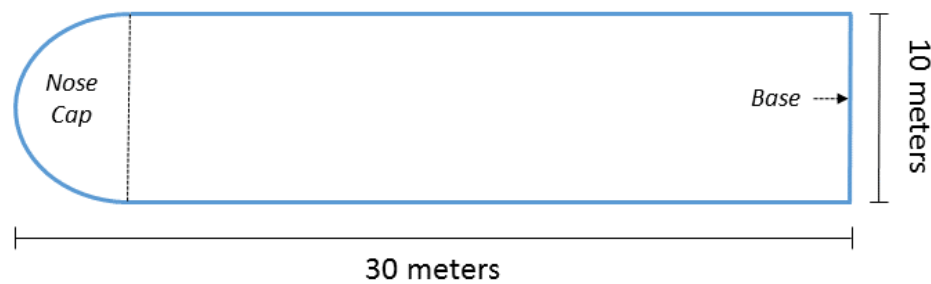

Figure 4: Mid L/D geometry.

C. Thermal Analysis Model

The thermal analysis was completed using the Fully Implicit Ablation and Thermal Response program (FIAT), a one-dimensional heat conduction code with ablation capabilities.[14] A heat flux boundary condition was applied to the heatshield surface, and an adiabatic boundary condition was assumed at the backface. The radiative and convective heat fluxes were specific to the vehicle trajectory, which included an aerocapture and entry phase, and were computed at the stagnation point. The convective and radiative heat fluxes are based on two-dimensional (2-D) axisymmetric LAURA and HARA computational aerothermodynamic solutions.[15] The heat flux for each vehicle is shown in Figure 5. Each heat flux is normalized with respect to the maximum heat flux during the Mid L/D aerocapture trajectory. The heating profile shown includes both the radiative and convective components and is separated into the aerocapture and entry trajectories. In both cases, aerocapture is a more severe heat flux over a shorter duration.[6] The Mid L/D vehicle has a longer entry portion of flight, a direct result of the shallower decent angle. For this study, the heat loads for the HIAD rigid nose had a factor of safety of 1.5 and 1.4 for the radiative and convective components, respectively.[7] The Mid L/D loads did not have a factor of safety applied.

American Institute of Aeronautics and Astronautics
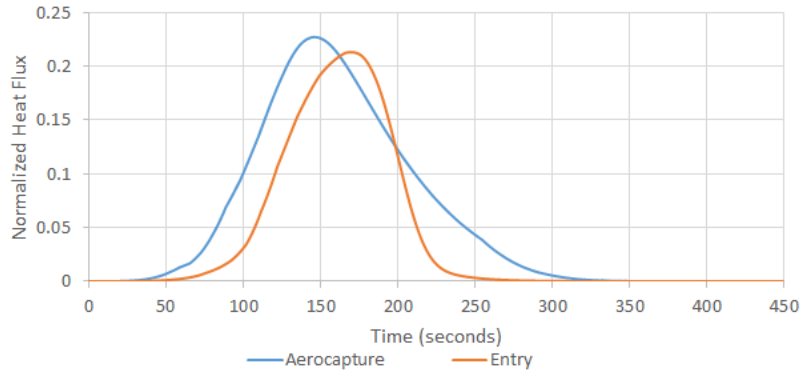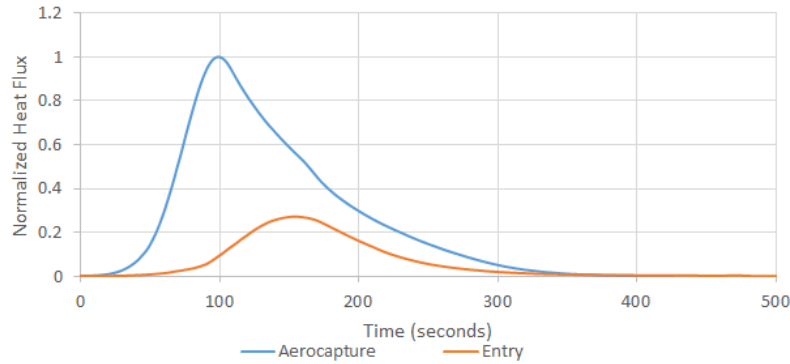
Figure 5: Normalized heat flux for the (a) HIAD and (b) Mid L/D vehicles, with respect to the maximum Mid L/D heat flux for aerocapture.

D. Structural Analysis Model

The structural analysis was performed using the Nastran[16] finite element software to determine the dimensions of the structural members which resulted in minimum weight given the aerodynamic and gravitational loads. The constraints included the material stress limit and critical buckling load. Similar meshing strategies were used for both the HIAD rigid nose and Mid L/D finite element models. For each specific vehicle, the same mesh was used for both the ablative TPS and hot structure design analyses. For the HIAD rigid nose, the element size was kept constant in the circumferential direction, while in the radial direction, node biasing was employed in order to obtain a finer mesh near the nose tip. Quadrilateral elements were used for the entire mesh with the exception of the inner ring of elements connecting to the node at the center. Triangle elements were used in this section. The mesh used with these two features highlighted is shown in Figure 6. The triangle elements are in red, while the quadrilateral elements are shown in black. The Mid L/D was meshed in a similar manner. The cylindrical section used quadrilateral elements of equal sizing, and the mesh of the hemispherical nose consisted of quadrilateral and triangular elements with radial biasing of the nose spacing near the nose tip. The element sizing was driven by convergence of the results with the coarsest mesh possible to facilitate quicker analysis times. The ablative TPS design was modeled entirely with shell elements as a symmetric sandwich composite with IM7 facesheets and an 5052 alloy hexagonal aluminum honeycomb core. The PICA was modeled as a non-structural mass distributed evenly across the entire model, for both the HIAD rigid nose and Mid L/D geometries. The hot structure designs were modeled using a stiffened skin approach, with both designs using shell elements for the skin. Both the skin and the stiffeners were modeled using approximated in-plane isotropic properties for ACC-6. In each model, the OFI TPS was modeled as a non-structural mass uniformly distributed over all the shell elements.

American Institute of Aeronautics and Astronautics

Quadrilateral elements outlined in **BLACK**
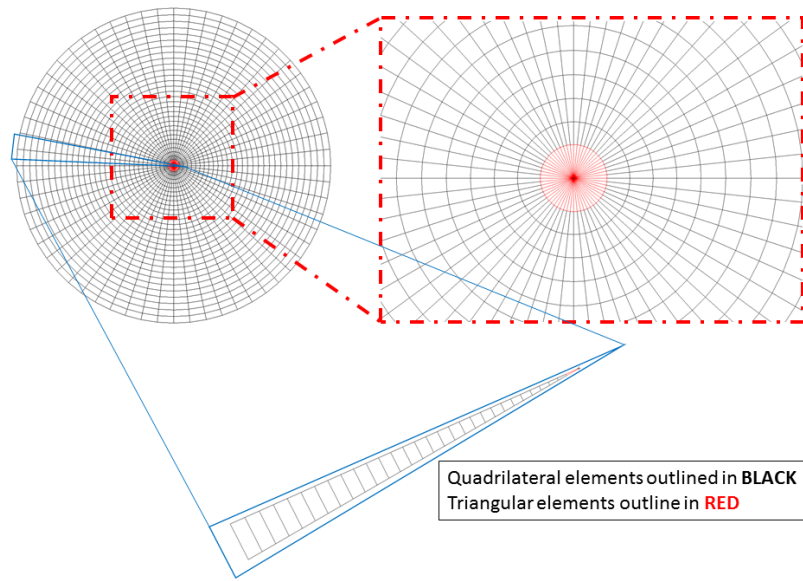Triangular elements outline in **RED**

Figure 6: Finite element mesh of HIAD rigid nose.

Both vehicle architectures face two structural loading cases, Earth launch and Mars entry. For the HIAD rigid nose, the Earth launch load case consists only of gravity loads. Pressure loads are not appropriate as the entire vehicle is contained within a shroud on the launch vehicle. For Mars entry, both a uniform pressure load and a gravity load are applied to the HIAD rigid nose. The pressure load is applied uniformly across the nose cap representing a zero degree angle of attack entry into the atmosphere at Mars.

The Mid L/D vehicle is designed to be launched without a shroud[6] and therefore, the Earth launch case consisted of both a pressure load and a gravity load.[8,9] A five-degree angle of attack for the vehicle at launch was determined to be appropriate and the pressure load is applied accordingly. For the Mars entry case, the application of gravity loads is not necessary due to the use of inertial relief for the boundary condition. Thus, only a pressure load is applied to the vehicle. The angle of attack for entry is fifty-degrees. Each of these loadings can be seen in Figure 7. Both pressure loads where computed using the modified Newtonian sine-squared law.[8] This method to compute the pressure load is considered a reasonable approximation for determining hypersonic aerodynamics.

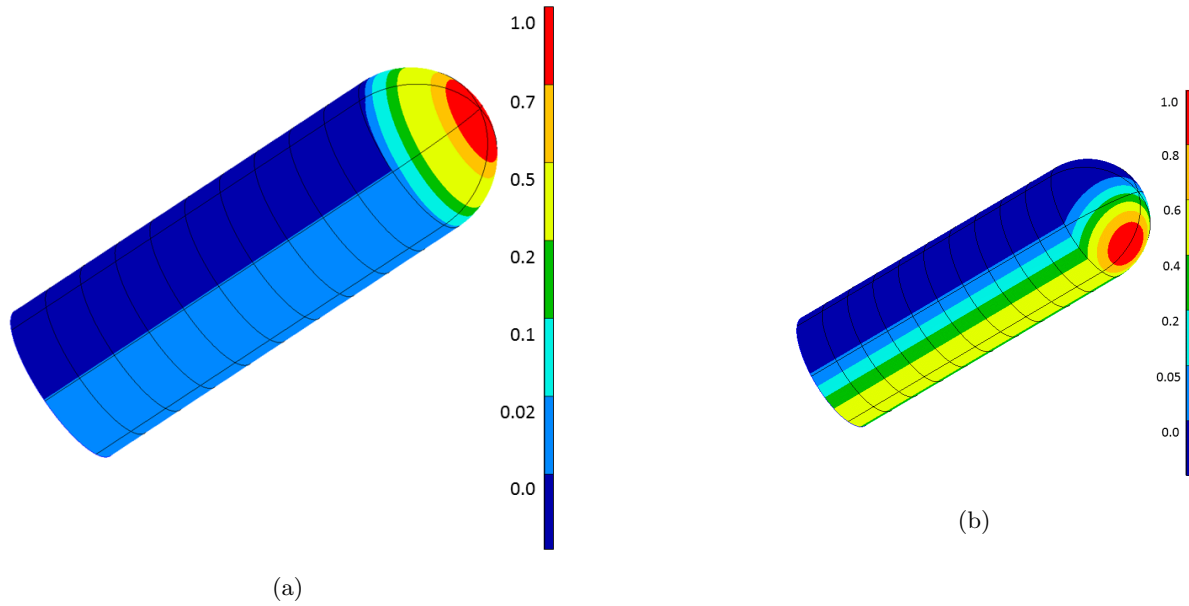American Institute of Aeronautics and Astronautics

Figure 7: Normalized Mid L/D pressure loads for (a) launch and (b) entry.

The boundary conditions used for the two vehicle configurations differed significantly, not only due to the differences in geometry, but also due to the Mid L/D design modeling the entire vehicle, while the HIAD rigid nose was only modeling a portion of the entire vehicle. For both vehicle configurations, when analyzing the ablative TPS design and the hot structure design, the same boundary conditions are used for each individual vehicle.

The HIAD rigid nose was clamped around the outer edge at the base of the nose. This configuration was selected to approximate the condition found at the attachment ring connecting the rigid nose to the rest of the vehicle. The assumption that this would be a clamped connection is considered valid for this analysis purpose due to the large mass of the rest of the vehicle when compared with the mass of the rigid nose section. Due to this approach, the same boundary conditions would appropriately model both the launch and entry loading conditions.

The boundary conditions for the Mid L/D model were different for launch and entry. For launch, a clamped boundary condition was applied to the base of the vehicle at locations coinciding with the ends of the longitudinal stiffeners. For entry, all constraints on the base of the model are removed and inertial relief is applied to create the opposing forces necessary for the static analysis of a structure moving through space. In each loading condition, the payload was included as multiple point masses at the center of the cylindrical body.

III.   Optimization Approach

The optimization for the thermal and structural analysis portions was conducted in an iterative approach because the thermal analysis required inputs that were outputs from the structural analysis (structural material thicknesses) and the structural analysis required the TPS thickness output from the thermal analysis as an input. Specifically, the interconnected inputs and output for the ablative TPS design were the thicknesses of the aluminum honeycomb and the composite facesheet and the thickness of the PICA. The thickness of the structural components are inputs into the FIAT sizing analysis for the PICA. In turn, the PICA thickness is used to derive the non-structural mass of the vehicle used during the Nastran analysis. The hot structure design was related similarly, with the ACC-6 thickness and OFI thickness replacing the aluminum core and composite facesheets and PICA, respectively. However, the interconnected inputs and outputs were not design drivers in either case and convergence was reached within three iterations in all cases.

American Institute of Aeronautics and Astronautics

A. Thermal Design

The thermal analysis was used to optimize the thickness of the TPS for each design. The design variables were the OFI thickness and the PICA thickness for the HIAD rigid nose and Mid L/D, respectively. The minimum thickness of the insulation required to satisfy a temperature constraint at a material interface given convective and radiative heat fluxes were determined by the thermal analysis. The insulation was sized to survive both aerocapture and entry, assuming no jettison of the heatshield. The temperature constraints at the material interfaces for each design and vehicle combination are shown in Table 1. The temperature constraint placed on the RTV-560 bondline was based on previous Mars entry, decent, and landing studies.[6] Even though Nextel can perform at much higher temperatures,[17] the Nextel constraint was chosen as a temperature which would be reasonable for the interior structure on both vehicles. The composite facesheets for the ablative TPS design were modeled as MJ55, which has very similar properties to IM7. In each case, the objective function was to minimize the TPS thickness, thus minimizing the weight.

Table 1: Thermal sizing temperature constraints

	HIAD Rigid Nose	Mid L/D
Ablative TPS Design	300°C at RTV-560/PICA interface	300°C at RTV-560/PICA interface
Hot Structure Design	150°C at Nextel Fabric	150°C at Nextel Fabric

B. Structural Design

For the structural optimization of each vehicle, both the number and arrangement of stiffeners was varied, as well as the optimization of stiffener dimensions (height and width) and skin thickness. The constraints used to size each vehicle included the buckling load limit and the material stress limit. For the HIAD rigid nose, a knockdown factor of 0.26 was also placed on the buckling load. This knockdown factor was based on empirical formulas for the buckling of a stiffened shell based on geometry and material property values.[18] The optimization technique used was a gradient-based search algorithm with an objective to minimize the total weight. The static and buckling analyses performed were both linear analyses. For the HIAD rigid nose geometry, sixteen different stiffener combinations were optimized with a 1.4 factor of safety placed on the material limits and the linear theoretical buckling load. The optimal stiffener arrangement found in this set was then re-optimized with the same material limits, and a knockdown factor[7] on the buckling load. The Mid L/D vehicle was analyzed similarly. Twenty-four different stiffener combinations were optimized according to material stress limits and the theoretical buckling load, no additional knockdowns or factors of safety were added. The optimal design from this group was then chosen as the optimal design.

IV.   Results

The figures of merit determined for this study were areal density and total thickness. In order to compare potential future designs across a range of sizes, the areal density was computed rather than mass or weight. In this study, the areal density reported includes the sized structure and insulation. The areal density allows a direct correlation and comparison of the vehicle mass. As mass is a key cost and design driver in space vehicles, this was considered the primary figure of merit. Thickness was also compared in order to characterize potential volume savings that one design might present over another. The volume savings provides additional payload capacity or a reduced vehicle size. Additionally, the reduction in thickness could lead to a favorable shift in the center of gravity of the vehicle which impacts the control system of the vehicle.

A. HIAD

The HIAD rigid nose showed a 65% reduction in thickness for the optimized hot structure design as compared to the ablative TPS design. The results are summarized in Table 2 and a visual representation of the two design layups is given in Figure 8. The HIAD rigid nose ablative TPS design did not include stiffeners. The loading conditions for this study led to a minimum gauge design for the composite sandwich. Therefore, the inclusion of stiffeners would not reduce the weight. The hot structure design was stiffened with blade stiffeners, which led to an 18% reduction in weight from an unstiffened hot structure design. The height and width of the stiffeners were optimized during the structural analysis and they were offset to the inner

American Institute of Aeronautics and Astronautics

side of the skin. The optimum stiffener arrangement included twelve longerons equally spaced and ten rings, also equally spaced, but following the nose biasing of the elements. The arrangement of the stiffeners in black, laid over the light green elements is shown in Figure 9. The rings were identically sized and found to be 2.159-millimeters square, which was the minimum gauge for the ACC-6 material. The longerons were also identically sized and found to be 8.411-millimeters in height and 8.4092-millimeters in width. Sixteen different stiffener arrangements were optimized, and the minimal weight design was selected from these arrangements. The twelve longerons and ten rings arrangement was the largest number of stiffeners tested. Expanding to higher numbers of stiffeners was deemed impractical for this study due to the geometry of the rigid nose and spacing of the stiffeners. Throughout all the results, the longerons had a greater effect in stiffening the structure than the rings.

Table 2: HIAD rigid nose thickness summary

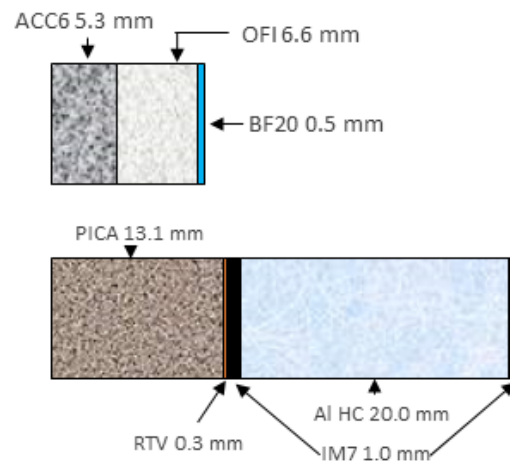| Ablative TPS Design	
PICA Thickness	13.14 mm
IM7 Facesheet	1.00 mm
Al Honeycomb	20.00 mm
RTV-560	0.30 mm
Total	35.44 mm
Hot Structure Design	
OFI Thickness	6.61 mm
ACC6 Thickness	5.25 mm
BF20 Thickness	0.5 mm
Total	12.36 mm

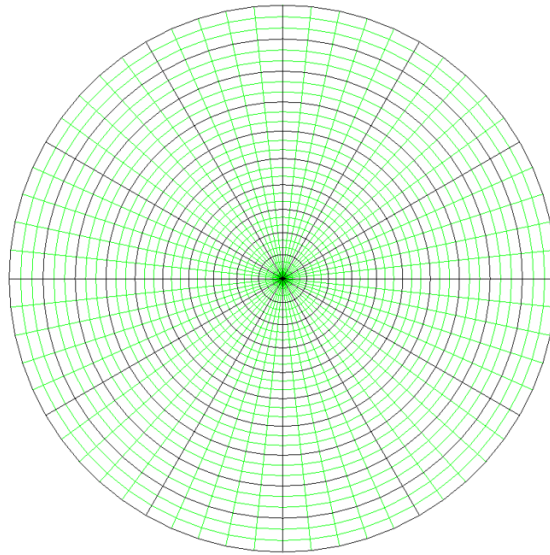Figure 8: Visual representation of HIAD nose cap thickness.

Figure 9: Optimum stiffener arrangement of hot structure HIAD rigid nose.

The areal density of the ablative TPS design was 8.53 kg/m^2 and the area density for the hot structure design was 10.07 kg/m^2. This corresponds to a 15% increase in areal weight for the hot structure design as compared to the ablative TPS design. While the hot structure design of the nose cap led to an increase in areal density, the overall increase in vehicle weight will be small.

B.   Mid L/D

The optimized Mid L/D aeroshell was found to have a 66% reduction in thickness for the hot structure design as compared to the ablative TPS design. The results are summarized and a visual representation is given later in this section. Unlike the HIAD rigid nose, for the Mid L/D vehicle both the ablative TPS and hot structure designs are stiffened. The ablative TPS design was stiffened with six rings and eight longerons, both modeled as IM7 material. Following the work of Lane[8] and Ahmed,[9] the cylindrical body and nose cap were divided into six shell sections for individual skin thickness optimization. The rings were divided into three groups for sizing the dimensions and all of the longerons were sized together. The division of the shell sections and placement of the rings and longerons can be seen in Figure 10. The dimensions for the honeycomb core and laminate thickness for each section of the optimized design is listed in Table 3.[9]
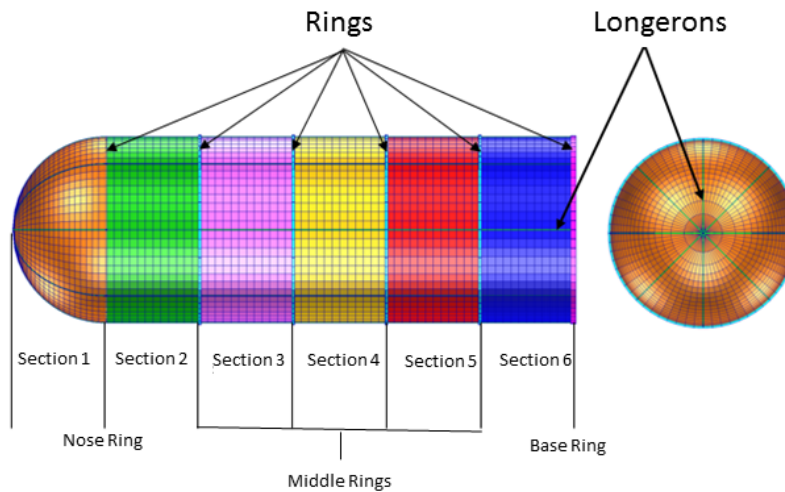

Figure 10: Shell sections and stiffener arrangement of Mid L/D ablative TPS design.[9]

American Institute of Aeronautics and Astronautics

Table 3: Optimized dimensions for the composite sandwich Mid L/D shell sections

	Section 1	Section 2	Section 3	Section 4	Section 5	Section 6
Core Thickness (mm)	20.0	20.0	33.4	31.0	29.8	94.8
Laminate Thickness (mm)	1.0	1.0	4.4	8.8	13.7	20.0

Channel stiffeners were used for the ablative TPS and hot structures Mid L/D aeroshell designs. The stiffener sizing consisted of optimizing the four cross-sectional dimensions shown in Figure 11,which is found in the Nastran documentation.[16] The labels in Figure 11 correspond to the dimensions listed in Table 4.
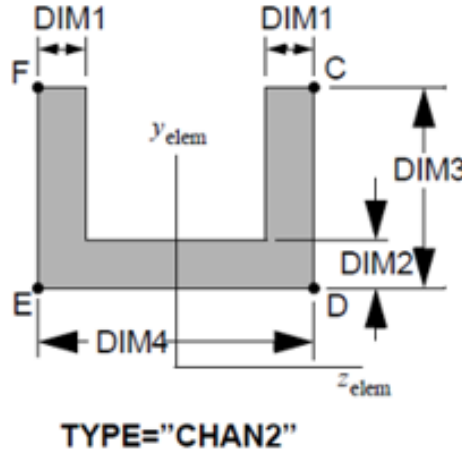

Figure 11: Channel stiffener used for Mid L/D vehicle.

Table 4: Optimized stiffener dimensions for Mid L/D ablative TPS design

	DIM1	DIM2	DIM3	DIM4
Longerons (mm)	6.7	8.9	55.1	71.6
Nose Ring (mm)	7.3	9.9	59.6	81.1
Middle Rings (mm)	10.7	14.4	300.0	157.2
Base Ring (mm)	10.8	37.5	300.0	300.0

The hot structure design was stiffened with eleven frames and eight longerons. The stiffeners were divided into longerons, nose ring, middle rings, and base ring to be optimized. However, a uniform skin thickness of 6.35 millimeters was applied for the hot structure design. This design also used the channel dimensions and the optimized values are found in Table 5, with the labels corresponding to Figure 11. Manufacturing considerations were not included for the stiffener dimensions in Tables 4 and 5.

Table 5: Optimized stiffener dimensions for Mid L/D hot structure design

	DIM1	DIM2	DIM3	DIM4
Longerons (mm)	5.0	5.0	40.0	40.0
Nose Ring (mm)	5.0	5.0	40.0	40.0
Middle Rings (mm)	5.0	6.3	300.0	72.9
Base Ring (mm)	28.4	15.1	300.0	177.8

The thermal analysis was run using the minimum skin thickness of the six shell sections for the ablative TPS design as this is the most conservative approach for the sizing. It was determined that changing the core

American Institute of Aeronautics and Astronautics

and facesheet thicknesses had an insignificant impact to the thermal response of the design. A comparison of the total thickness between the ablative TPS and hot structure designs is shown in Figure 12. The minimum core and facesheet thickness from the six shell sections is listed for the ablative TPS design in a comparison found in Table 6.

Table 6: Optimized Mid L/D aeroshell thickness summary

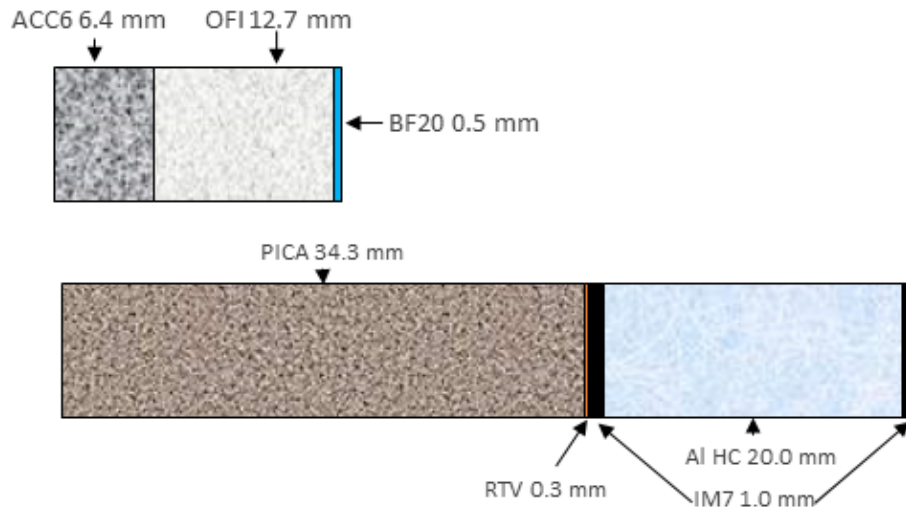| Ablative TPS Design	
PICA Thickness	34.3 mm
IM7 Facesheet	1 mm
Al Honeycomb	20 mm
RTV-560	0.3 mm
Total	56.6 mm
Hot Structure Design	
OFI Thickness	12.68 mm
ACC6 Thickness	6.35 mm
BF20 Thickness	0.5 mm
Total	19.53 mm

Figure 12: Visual representation of the Mid L/D aeroshell thickness.

The areal density of the ablative TPS design was 40.9 kg/m^2, and the areal density for the hot structure design was 13.6 kg/m^2. This corresponds to a 67% reduction in areal weight for the hot structure design as compared to the ablative TPS design. The areal density for the ablative TPS design includes the variation in skin thickness for the six shell sections.

V. Concluding Remarks

The purpose of this work is to study a hot structure design as a feasible and attractive alternative to state-of-the-art ablative TPS technology for a Mid L/D aeroshell and HIAD nose cap for Mars entry. The development of vehicles that can deliver large payloads to Mars is essential for successful human exploration. This study investigated two different vehicles capable of delivering large payloads to Mars, a Mid L/D concept and the nose cap of a HIAD concept. The differences in weight and volume of the aeroshell and nose cap are compared for the hot structure and ablative TPS designs.

The hot structure and ablative TPS designs were sized for each vehicle subject to structural and thermal

American Institute of Aeronautics and Astronautics

loads appropriate to its specific architecture. The insulation and structure for each design were independently sized for thermal and structural launch and entry loads. The figures of merit for comparing the hot structure and ablative TPS designs are the areal weight and thickness. The hot structure design provides a reduced thickness for the Mid L/D aeroshell and HIAD nose cap compared to the ablative TPS design. The hot structure design exhibits a reduced areal density for the Mid L/D aeroshell, while the HIAD nose cap exhibited an increase in areal density for the hot structure design. These conclusions are specific to the designs presented in this paper, including the geometry, loads, and modeling features used.

The preliminary design and analysis indicates that a CMC aeroshell or heat shield for a Mars entry vehicle is a feasible alternative to an ablative TPS design with potential volume and weight savings depending on design factors such as geometry, loads, and mission requirements. This area of study would benefit from future work to better understand the hot structure design by increasing the analysis fidelity and validating with experimental data.

Acknowledgments

References

[1]Glass, D. E., "Ceramic Matrix Composite (CMC) Thermal Protection Systems (TPS) and Hot Structures for Hypersonic Vehicles," *15th AIAA Space Planes and Hypersonic Systems and Technologies Conference, AIAA 2008-2682*, 2008.

[2]Blosser, M. L., *Advanced Metallic Thermal Protection Systems for Reusable Launch Vehicles*, Ph.D. Dissertation, University of Virginia, Charlottesville, VA, May 2000.

[3]Wright, M. J. et al., "Sizing and Margins Assessment of the Mars Science Laboratory Aeroshell Thermal Protection System," *41st AIAA Thermophysics Conference, AIAA 2009-4231*, 2009.

[4]Edquist, K. T., Dyakonov, A. A., Wright, M. J., and Tang, C. Y., "Aerothermodynamic Design of the Mars Science Laboratory Heatshield," *41st AIAA Thermophysics Conference, AIAA 2009-4075*, 2009.

[5]Willcockson, W. H., "Mars Pathfinder Heatshield Design and Flight Experience," *Journal of Spacecraft and Rockets*, Vol. 36, No. 3, May-June 1999, pp. 374–379.

[6]Dwyer, A. M. et al., "Entry, Descent and Landing Systems Analysis Study: Phase 1 Report," *NASA TM-216720*, 2010.

[7]Bose, D. M. et al., "The Hypersonic Inflatable Aerodynamic Decelerator (HIAD) Mission Application Study," *Aerodynamic Decelerator Systems Technology Conference and Seminar, AIAA 2013-1389*, 2013.

[8]Lane, B. M. and Ahmed, S. W., "Parametric Structural Model for a Mars Entry Concept," 2016 NASA-TM, under review.

[9]Ahmed, S. W. and Lane, B. M., "Finite Element Modeling and Analysis of Mars Entry Aeroshell Baseline Concept," 2016 NASA-TM, under review.

[10]Samareh, J. A. and Komar, D. R., "Parametric Mass Modeling for Mars Entry, Descent and Landing System Analysis Study," *49th AIAA Aerospace Sciences Meeting*, No. AIAA 2011-1038, January 2011.

[11]Agrawal, P., Prabhu, D., Milos, F. S., and Stackpoole, M., "Investigation of Performance Envelope for Phenolic Impregnated Carbon Ablator (PICA)," *SciTech 2016*, No. AIAA 2016-1515, January 2016.

[12]Walker, S. P. et al., "A Multifunctional Hot Structure Heatshield Concept for Planetary Entry," *International Space Planes and Hypersonic Systems and Technologies Conference, AIAA 2015-3530*, 2015.

[13]Daryabeigi, K., Cunnington, G., Miller, S., and Knutson, J. R., "Combined Heat Transfer in High-Porosity High-Temperature Fibrous Insulations: Theory and Experimental Validation," *AIAA 2010-4660*, June 2010.

[14]Chen, Y. K. and Milos, F. S., "Ablation and Thermal Response Program for Spacecraft Heatshield Analysis," *Journal of Spacecraft and Rockets*, Vol. 36, No. 3, May-June 1999, pp. 475–483.

[15]Brune, A. J., West, IV, T. K., Hosder, S., and Edquist, K. T., "Uncertainty Analysis of Mars Entry Flows over a Hypersonic Inflatable Aerodyanmic Decelerator," *Journal of Spacecraft and Rockets*, Vol. 52, No. 3, May-June 2015, pp. 776–788.

[16]Anon, *MSC Nastran 2012.2 Quick Reference Guide*, MSC Software Corporation, Santa Ana, CA, 2012.

[17]DeMange, J. J., Dunlap, P. H., Steinetz, B. M., and Drlik, G. J., "An Evaluation of High Temperature Airframe Seals for Advanced Hypersonic Vehicles," *NASA TM-215043*, 2007.

[18]Bushnell, D., Almroth, B. O., and Sobel, L. H., "Buckling of Shells of Revolution with Various Wall Constructions," *NASA-CR-1050*, 1968.